論　文

J. Jpn. Soc. Soil Phys.
土壌の物理性
No. 83, p. 3～16 (2000)

Crack Pattern Analysis For Moisture Prediction In Drying Dredged Material

P. O. Bodun[1], S. Shibusawa[1], A. Sasao[2] and K. Sakai[2]

[1] Graduate School of Bio-Applications and Systems Engineering, Tokyo University of Agriculture and Technology
[2] Agricultural and Environmental Systems Engineering, Faculty of Agriculture, Tokyo University of Agriculture and Technology, 3-5-8 Saiwai-cho, Fuchu 183, Japan

Abstract

During the drying process, dredged sludge undergoes the process of shrinkage that typically begins at the surface, followed by the formation of three dimensional networks of planar cracks that break the sludge into fragments (clods) of various sizes. This paper presents the description of the crack networks by the processes of image analysis for describing the sludge response to change in moisture content with the morphological features of the cracks and clods during the drying process. From analysis, all crack features increased with a decrease in sludge moisture content ; the clod features, except the number of clods, decreased with a decrease in sludge moisture ; while the crack elongation remain fairly constant with a decreasing sludge moisture content. At 8% d. b, the equilibrium moisture content, the crack area was 0.96 times as large as the clod area ; and the crack-clod ratio had a good logarithmic relationship with the sludge moisture content. The crack pattern was found to depend on the sludge drying rate and the moisture level within the sludge body.

Key words : sludge drying, image processing, crack-clod morphological features, and moisture content

1. Introduction

Water quality improvement and pollution control have been the subject of consideration in lake Kasumigaura (Japan) in the recent years, and dredging the lake bottom sludge has been implemented as an important option in the rapid improvement of the lake water quality. For environmental protection, the dredged sludge from the lake bottom is placed in a confined disposal yard of about 270 ha on paddy fields borrowed from farmers. The sludge retains high moisture for a very long time, presents problems in mobility on the ground surface, and makes quick reclamation difficult, which eventually lengthen the drying time, and increase the cost of managing the borrowed fields.

In order to accelerate the sludge drying speed, mixing and pulverization of the dredged sludge in situ was considered, which required mechanical handling. To overcome the mobility and workability problems during these operations, an integrated sludge handling system (Shibusawa *et al.*, 1996), which consists of three main stages were planned. The stages are : (i) surface information sensing for sludge moisture prediction, (ii) trafficability and workability studies on the soft sludge surface, and (iii) the handling stage, which involves measures to be taken in accelerating the sludge drying speed. In this paper, attention is focused on the possibility of using the surface information developed during the drying process to predict

the sludge moisture condition in correspondence with the relationship between the sludge cone index and moisture content developed by Nonaka (1997).

Two significant features are developed during the sludge drying process : textural variation accompanied with color changes ; and the development of three-dimensional crack networks on the sludge surface. Textural variation has been analyzed for sludge moisture prediction, (Bodun, *et al.*, 1999), but the prediction model could only be applied at high moisture content (above 150% d. b). Therefore, means of predicting the sludge condition to a much lower moisture content resulted in the analysis of the three-dimensional crack networks. In sludge drying, crack is considered an important sludge surface information, because the volume and its configuration controls the acceptance, transmission and storage of moisture, and the movement of gases within the sludge body, thus playing an important role in the rapid evaporation of moisture from the sludge body.

When sludge materials is allowed to dry through natural evaporation, in due time, an irregularly spaced cracks tends to appear on the surface. As evaporation continues, these cracks gradually expand and deepen such that regions of sludge between the cracks temporally vary from separate, free standing, irregular structures of roughly similar size and shape. This process of crack formation is self-generating, in the sense that once it begins, drying and shrinkage can cause it to extend from one side to another and some may extend indefinitely. Scott *et al.*, (1986) have described soil crack networks in terms of its density and orientation, and found that the distribution of inter-crack distances appeared to be exponential. O'Callaghan *et al.*, (1973) have developed a quantitative means of measuring properties of soil cracking patterns. Horgan (1998), has used mathematical morphology to analyze soil structure from soil images, including soil cracking pattern, with suggestion that this method could be used in comparing cracking pattern in different soil types. Waller & Wallender (1993) have made qualitative and quantitative observations of soil cracking behavior, they found that crack area follows a change in the soil bulk density, but they did not correlate the cracking and the ped size with the soil moisture content. Preston *et al.* (1997) have also used fractal dimensions to quantify the complex geometry of soil cracking pattern, and they found that a significant relationship exists between the soil clay content and the fractal dimensions of the cracks. Ringrose-Voase & Bullock (1984) have developed an automatic recognition technique based on shape factors for discriminating and measuring the properties of pore classes. Ringrose-Voase (1987, 1990), Ringrose-Voase & Nys (1990) have all used image analysis technique to make qualitative description of pores in the soil horizon. The work of Murphy *et al.* (1977) and Moran *et al.* (1989) have also involved the application of image analysis technique for rapid analysis of soil pore structures. Several other research work reported in Bronswijk (1991) have been on the measurement of crack volume with different methods, while Bronswijk himself has investigated the relationship between vertical soil movements, cracking and water loss in the fields. He found that the ratio of water loss to three-dimensional volume shrinkage was as high as 0.80, without actually measuring the crack features, only the volume of shrinkage in the cracking soil.

Based on the morphological properties of the crack networks, and the series of past work, centered mainly on measuring the crack pattern complexity in terms of its fractal dimensions and shrinkage measurements in cracking soil, without taking the crack and clod morphological features into consideration. This research work therefore focus on the measurements and the use of the crack and clod morphological features to describe and

compare the crack pattern variation on different sludge image with changes in the sludge moisture content. The objectives of this research work are therefore :

(i) Analyze the crack formation pattern, to extract the crack and clod morphological features with changes in the sludge moisture content.

(ii) With the extracted morphological features, to develop a regression model for the sludge moisture prediction.

2. Materials and Methods

2.1 Experiments

Using the dredged sludge from Lake Kasumigaura, two experiments were conducted in a vinyl pipe house. The first experiment (A) was conducted from the 7th of May 1996 to 29th of May 1996. During this period, the vinyl pipe house average daily dry temperature was 25℃, and the average relative humidity was 79%. At the commencement of the experiment, the initial sludge moisture content was 458% (d. b), and when there was no further drying (only re-absorption of moisture), at sludge moisture content of 8% (d. b), the experiment was terminated. The second experiment (B) was conducted from 12th of November 1997 to 16th of January, 1998, in the vinyl pipe house, with the initial sludge moisture content of 398% (d. b), daily average dry temperature of 13℃, and the average relative humidity of 60.58%. At the 2nd week of the experiment, electric heater was used in the vinyl pipe house when it was discovered that the sludge surface became iced. When the sludge clods crumbling begins at moisture content of 67% d. b, the experiment was terminated. Experiments A and B differs in the sludge batch used, and the environmental condition in which they were conducted. In each experiment, dredged sludge was dried in an acrylic plastic box of dimensions 0.5×0.5×0.15 m at an initial depth of 0.1 m. The depth 0.1-m was chosen partly due to the box size, and the zone that is the most active region where the surface information, crack pattern, varies rapidly with moisture content. At each time of the experiment, the drying box was heat insulated, water sealed on the sides. This was done to make the temperature distribution uniform, and to make the condition a little similar to the natural condition in the disposal yard, where sites have sealed ridges and no sub-soil drainage could take place, except allowing for moisture dissipation at the top surface. At the deposition of wet sludge into the acrylic box, the sludge initial moisture content (dry basis), dry mass, and the initial wet mass were determined. Daily surface images of the drying sludge were captured with digital camera (Fujix DS 200), in an illuminated chamber. Image capturing conditions such as height of capturing (0.5 m), position, lens aperture and lightning were kept constant during the experiments. Concurrently daily weights of the acrylic plastic box and its content were measured with electrical balance (EP 20 KA). Experiment A was dried to its equilibrium moisture content, and no crumbling of cracks was observed throughout, while experiment B was terminated when the crumbling of the surface cracks began, it did not gets to its equilibrium moisture content. From the daily weights, dry mass, and the initial moisture content data of the sludge body, the sludge daily moisture contents were calculated. Fig. 1 presents the original image of one of the sludge surface (from experiment B) showing the sludge tex-

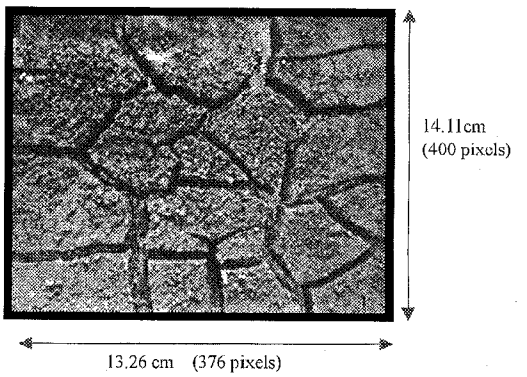

Fig. 1 Original image of the sludge surface at moisture content of 161% d.b.

ture and the crack pattern at moisture content of 161% (d. b).

2.2 Image Processing

The resulting digital images from the two experiments were of a high resolution (512×512 pixels), with each pixel equivalent to 0.35 mm. The images, which were in color, were first converted to their gray level. On the images, certain pictorial features makes recovering of the cracks very difficult, light enters wide cracks, and sludge crumbling (especially in experiment B) disrupts their continuity. To make the processing feasible, each of the images from the two experiments was duplicated, with one kept as the original copy and the other one as duplicate copy. The duplicate copy of each image was placed side by side with its original copy, and was edited manually with Adobe Photoshop™ software to remove extraneous materials along the crack paths. During the editing of the duplicate copy, constant reference was made to the original copy to minimize error in the segmentation process. To save computer running time and avoid memory problems, each of the edited images were then reduced into a rectangular areas of 106×100 pixels (37.5 mm×35.3 mm), and were digitized, valued in the range 0-255 gray levels in a program coded in C++ for further analysis.

2.2.1 Image Binarization

An approach that was felt to be more intuitive for extracting the crack and clod morphological features was to consider the regions enclosed by cracks (clods) as ground, and the cracks as the object. A threshold value was set for each image by using the gray level histogram of each image matrix. Pixel values less than the threshold value was set to 1 (clod) and level at or above the threshold was set to 0 (crack). Fig. 2 shows the cracking pattern of the sludge image at moisture content of 161% (d. b). In order to recognize the various morphological features of each binary image, which could be used for describing the crack pattern, the use of pattern recognition technique was adopted. This involved the recognition of the morphological features of each of the image that continuously varying as the drying progresses. The morphological properties chosen were those that are independent of the image size and orientation (Ringrose-voase and Bullock, 1984). Cracks area and perimeter alone are not suitable individually for the measurement of the crack shape, because they are size dependent, hence they were combined to calculate the size independent shape characteristic called compactness. Calculating the crack elongation, which is also size independent and the angle of orientation, which depends on the image shape, carried out further crack description. From each of the sludge binary images, crack area, A, was estimated by counting the number of pixels within the crack regions, and crack perimeter, T, was estimated as a by-product of the crack length along the crack boundaries (Ioannis, 1995) by the relationship :

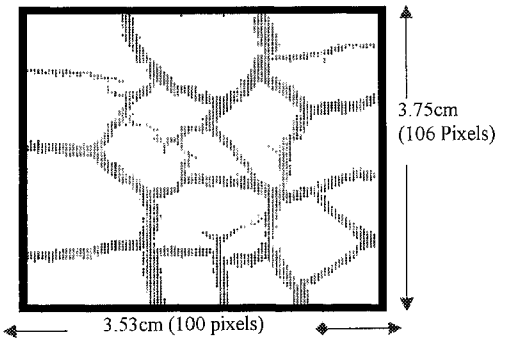

Fig. 2 The cracking pattern of the sludge surface at moisture content of 161% d. b.

$$T=\sum_i \sqrt{(X_i-X_{i-1})^2+(Y_i-Y_{i-1})^2} \quad (1)$$

Where :

X_i and Y_i are the coordinates of the crack boundaries pixels

The crack compactness, γ, angle of orientation, θ, and elongation, E, were estimated by the relationships stated by Ioannis (1995) as follows:

$$\gamma=T^2/4\pi A \quad (2)$$

Compactness measures the complexity of the crack shape, it increase with complicated

shapes, and as the shape deviate from a circle. For a disc, the value is 1. The crack angle of orientation, θ, is the angle between the crack major axis and the X axis. It measures the angle of crack displacement along the major axis in radian as follows :

$$\theta = \frac{1}{2} arctan \left(\frac{2\mu_{11}}{\mu_{20} - \mu_{02}} \right) \quad (3)$$

While the crack elongation, E, is the square root of the second moments along the major and minor axes of the crack. It is estimated by the relationship :

$$E = \sqrt{\frac{\mu_{20}\cos^2\theta + \mu_{20}\sin^2\theta - \mu_{11}\sin 2\theta}{\mu_{02}\sin^2\theta + \mu_{20}\cos^2\theta - \mu_{11}\cos 2\theta}} \quad (4)$$

Where :

μ_{02} is the crack variance at X axis.

μ_{20} is the crack variance at Y axis.

μ_{11} is the crack covariance at X and Y axes

Spherical and rectangular objects have an elongation of 1.

2.2.2 Clods Labeling

After the calculation of the crack shape characteristics on each of the binary images, clod labeling was performed to estimate the number of clod, and the area of each clod. Each of the sludge binary image matrix was scanned from left to right and from top to bottom by examining the neighboring pixels immediately to the left, t, above, r, top left diagonal, s, and top right diagonal, q, to the current pixel, p, to check their connectivity. The existence of an adjacent pair of pixels :

(p, t) where $p=0$ and $t=1$

indicates the boundary of a clod. A new clod is detected by the pair of adjacent pixels :

(t, p) where $t=0$ and $p=1$

And starting from these pairs, each of the image matrixes was traced in a clockwise direction. If p is 0, the next position is scanned, if p is 1, and all the other four neighbors listed above are zeros, then a new label is assigned to p. If only one of p neighbors is 1, its label is assigned to p, and if two or more neighbors of p are 1, one of their label is assigned to p, and a note of an equivalence is made. Following this process, the equivalent label pairs were sorted into their equivalence classes (Gonzalez and Woods, 1993), and a unique label is assigned to each class. Fig. 3 shows a sample of a labeled local area of the sludge surface image with its clods and crack features shown in Table 1.

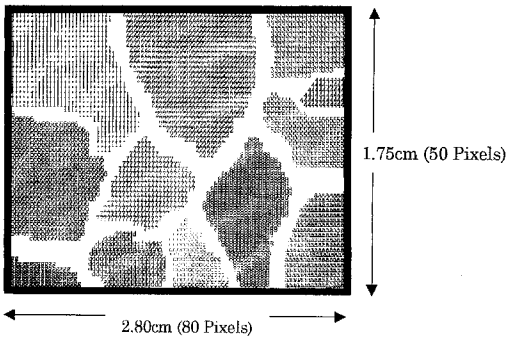

Fig. 3 A labeled local area of the sludge image at moisture content of 161% d.b.

Table 1 Statistics of the labeled sludge image in Fig. 3

	Clod 1	Clod 2	Clod 3	Clod 4	Clod 5	Clod 6	Clod 7	Clod 8	Clod a	Clod c	Clod d	Clod g
Area												
(Pixel)	644	772	247	61	218	529	290	430	252	137	185	85
(cm^2)	0.80	0.96	0.31	0.08	0.27	0.66	0.36	0.54	0.31	0.17	0.23	0.11
Perimeter												
(Pixel)	910.68	1,091.69	349.28	86.26	308.27	748.06	410.09	608.06	356.35	193.73	261.61	120.20
(cm)	32.15	38.54	12.33	3.05	10.88	26.41	14.48	21.46	12.58	6.84	9.23	4.24
Compactness												
	102.48	122.85	39.30	9.71	34.70	84.18	46.15	68.42	40.10	21.80	29.44	13.53

Crack-cold ratio=0.29 Average clod area=0.39 cm^2 Total clod area=4.78 cm^2 Crack area=1.38 cm^2

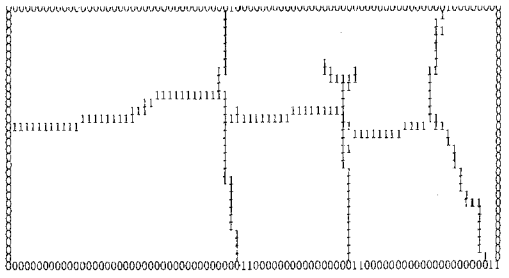

Fig. 4 Thinned structures of a local area of the sludge image at moisture content of 230% d.b.

From the labeled images, area of each clod, number of clods, clods perimeter, compactness, total clods area and the average clod area were estimated. From the results obtained, the crack-clod ratios were estimated for each of the image, as the ratio of the total crack area to the total clod area.

2.2.3 Cracks Thinning

Further processing of the sludge binary images were carried out to recover a thin line representation of the cracks in each image, from which values for crack widths and total crack lengths were obtained. An approach for representing the structural pattern of the cracks was accomplished by obtaining the medial axis of the cracks. In carrying out this operation, crack regions were reassigned the value 1, while the clod regions were reassigned value 0. Following which successive passes of the two basic steps thinning algorithm (Gonzalez and Wood, 1993) were applied to the crack points for peeling off the border pixels. Fig. 4 is a thinned structure of a local area in an image bordered by zeros.

Total crack lengths for each image was obtained by counting the number of pixels along the thinned crack lines. The crack width was obtained by updating the number of passes of the algorithm steps involved in reducing the largest crack width to a thin structure of a single pixel width. All the above processes were applied on all the images collected during the two experiments to extract the total crack lengths and widths.

3. Results and Discussion

In the two experiments, at the initial stage of drying, and before the formation of surface cracks, there was the initial phase of moisture extraction from the sludge pores, thus resulting in the sludge consolidation and reduction in the sludge volume. The pores which later serves as source of weakness for crack formation. From the results obtained in the two experiments, experiment A, took 22 days to dry from its initial moisture content of 458% d. b to the equilibrium moisture content of 8% d. b, corresponding to an average of 524.48 g of moisture lost per day. The first crack appeared on the sludge surface 5 days after the commencement of the experiment. Experiment B took 64 days to bring the sludge moisture content from its initial value of 398% d. b to 67.24% d. b, despite its initial lower moisture content and the use of electric heater in the vinyl pipe house when the sludge surface became solidified, leading to an average loss of 152.29 g of moisture content per day, with the first crack appearing 27 days at the moisture content of 271% d. b after the commencement of the experiment. In experiment A, high drying rate, caused by the relatively high temperature and humidity resulted in the earlier formation, and increase in crack properties, at high moisture content of 351% (d. b), consequently affecting the mean change in its compactness, 46.36 per day, and the average of total crack compactness, of 371.29. Experiment B has a mean change of 20.40 in its compactness per day, and average of total crack compactness of 272.76. On the other hand, the difference in the batch of sludge used for the experiments, and the effect of environmental conditions may have resulted in the earlier crumbling of the sludge clods in experiment B.

Qualitative view of the sludge surface image shows that the crack pattern differs at different moisture level in the two experiments. The number of crack appearing per unit area,

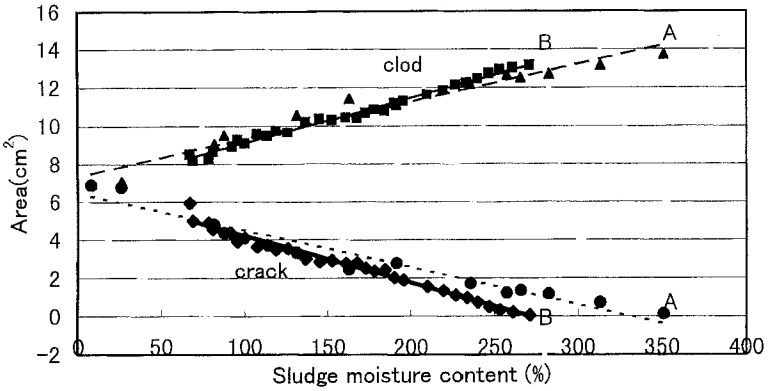

Fig. 5 The graph of crack and clod areas against the sludge moisture content.

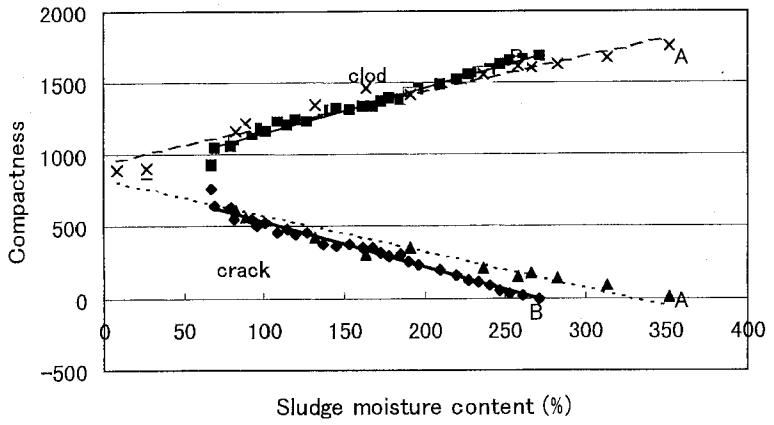

Fig. 6 The graph of crack and clod compactness against the sludge moisture content.

which is the crack density increased with a decrease in the sludge moisture content, which consequently affects the values of the crack and clod morphological features at different moisture content.

The pattern of cracks at the surface of a uniformly drying sludge appears as shown in Fig. 1. A set of polygons of roughly similar size and shape are formed as a result of clod displacement and further separation by the shrinkage process. Qualitative observations of the sludge surface shows that there were two distinct types of crack, the deep, straight, wide, and coarse cracks, extending from the sludge surface to the bottom of the drying box, and encompassing the sludge clods ; and the thinning, shallow cracks on the clods surface called micro cracks. The coarse cracks begins as a small fracture or micro cracks with shallow depths on the sludge clods, and gradually expands and increase in length and depth with a decrease in the sludge moisture content. The crack pattern, especially the clods size and shapes are the basic characteristics that are determined by the amount of clay (Preston *et al.*, 1997), the sludge moisture content, and the sludge drying rate.

Results of the analysis of all the images collected in the experiments are as shown in Fig. 5 for the cracks and clods area, and in Fig. 6 for the clods and cracks compactness. Cracks area increased with a decrease in the sludge

Table 2 Equations and the coefficient of determination of the crack area, compactness, length ; and clod area, and compactness against the sludge moisture content for experiment A and B

	Experiment A		Experiment B	
	Crack	Clod	Crack	Clod
Area	$Y=-0.020X+6.50$ $R^2=0.953$	$Y=0.020X+7.37$ $R^2=0.953$	$Y=-0.024X+6.67$ $R^2=0.976$	$Y=0.023X+6.73$ $R^2=0.988$
Compactness	$Y=-2.496X+830.29$ $R^2=0.953$	$Y=2.497X+940.74$ $R^2=0.953$	$Y=-3.133X+848.59$ $R^2=0.974$	$Y=3.158X+833$ $R^2=0.976$
Length	$Y=-26.907\ln(X)+159.53\cdots\cdots R^2=0.934$		$Y=-17.365\ln(X)+103.81\cdots\cdots R^2=0.781$	

X is the sludge moisture content (%) in the respective equations.
Y is the value of area, compactness, and length of cracks and clods in the respective equation.

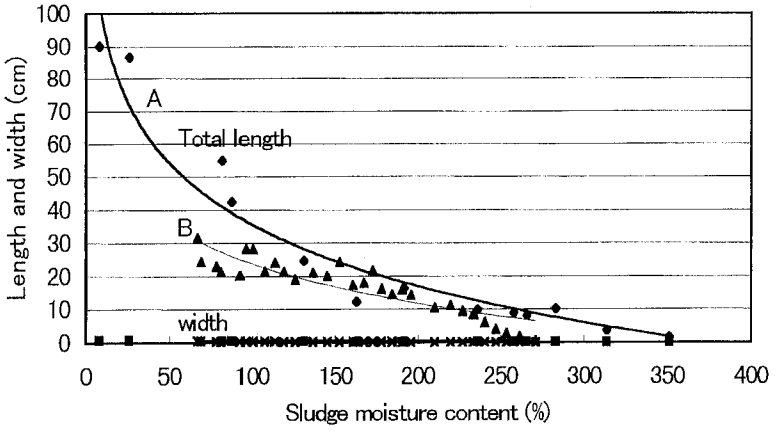

Fig. 7 The graph of crack length and width against the sludge moisture content.

moisture content, while the clods area decreased with a decrease in the sludge moisture content, at very low moisture contents, they both converge towards each other. In Fig. 6, the crack compactness increased with a decrease in the sludge moisture content, while the clod compactness decreased with a decrease in the sludge moisture content. During sludge drying, shrinkage, which is caused by the constant extraction of moisture from the sludge body, caused the formation of new cracks. Gradual, and horizontal displacement of the sludge clods resulted in the deepening and enlargement of the existing cracks, hence increasing the cracks area, their perimeters, and compactness, while causing a reduction in the clods area, perimeter, as well as their compactness value because of the consolidation process. Table 2 shows the equations and the coefficient of determination of the crack area, compactness, length, and clod area, and compactness against the sludge moisture content for experiment A and B.

Figure 7 and Fig. 8 shows the graphs of the crack length and width, and the plot of number of clods against the sludge moisture content respectively. The cracks length and width increased with a decrease in the sludge moisture content, but the increase in the crack width was negligible compared to the total crack lengths. Cracks length become unstable at low moisture contents because (i) during the

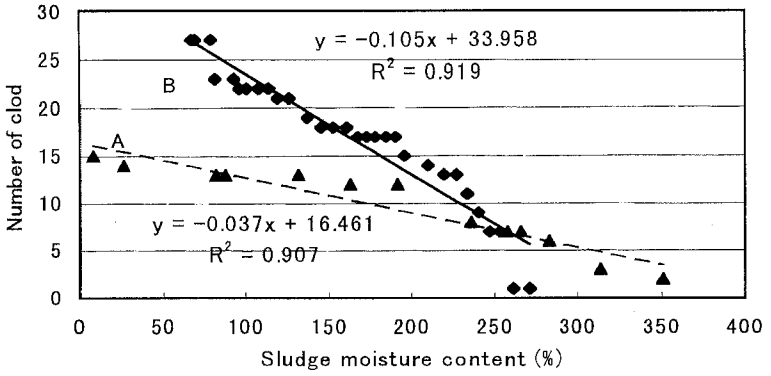

Fig. 8 The graph of number of clods against the sludge moisture content.

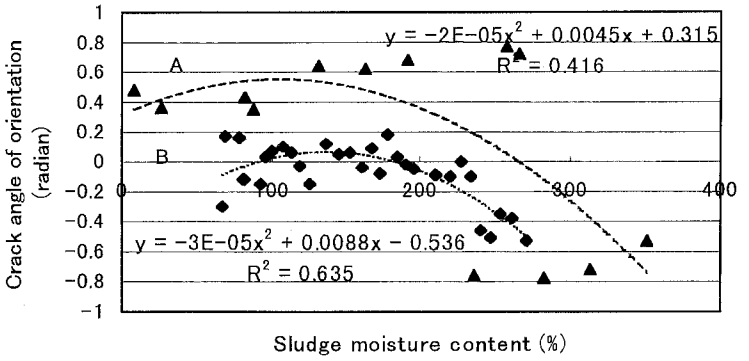

Fig. 9 The graph of crack angle of orientation against the sludge moisture content.

digitization process, micro cracks are sometimes disconnected. (ii) large difference in crack widths, especially between the coarse and the micro cracks, and the difference in crack widths at the crack junctions caused disconnection and sometimes deletion of the micro cracks after successive passes of the thinning algorithm. (iii) at low moisture contents, there is the difficulty in the separation of cracks from clods due to light that enters the wide cracks, crumbling of clod particles, and the development of micro cracks. In Fig. 8, constant degradation of the sludge structure as a result of moisture extraction led to the increase in the number of clods with a decrease in the sludge moisture content. Although experiment A and B were conducted using the same box size, there were fewer number of clods in experiment A compared to those in experiment B. On the clod geometry, individual clod vary in sizes, and they all show polygonal shapes with their edges rough or jagged.

Figure 9 and Fig. 10 are the graphs of the crack angle of orientation and elongation respectively. The relationship between the crack angle of orientation and the sludge moisture content exhibits a parabolic shape, and at a single value of the angle of orientation, there were two values of the sludge moisture content at moisture content below 200% d. b, and the R^2 are generally low in the two experiments. The angle of orientation increased from a negative value to a maximum positive value, remain constant for a short range of moisture contents, before gradually reducing to a lower values at low moisture contents. Crack elon-

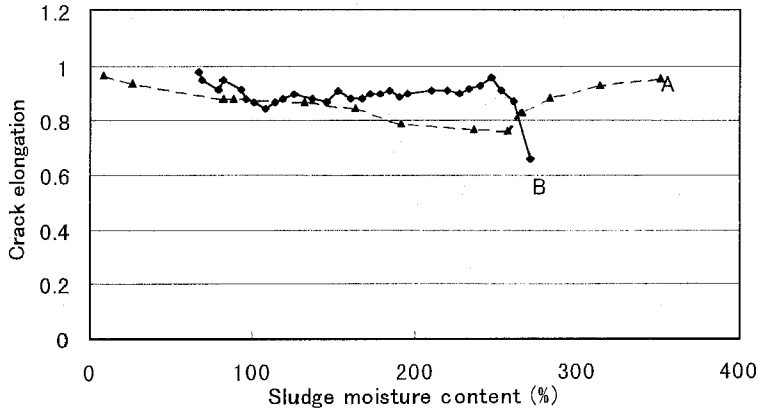

Fig. 10 The graph of crack elongation against the sludge moisture content.

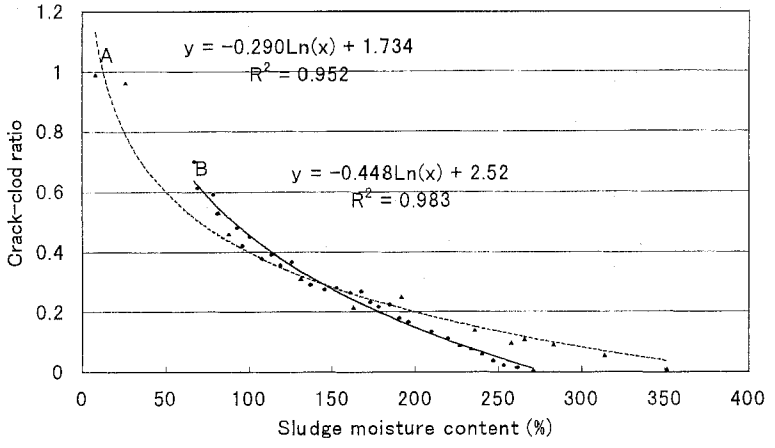

Fig. 11 The graph of crack —clod ratio against the sludge moisture content.

gation was virtually constant throughout the sludge drying period, except at the initial stage of the crack formation where little variation occurs. This result shows that the increase in the cracks length and width were gradual, with newly formed cracks following a repetitive pattern of the existing cracks.

The crack-clod ratio shown in Fig. 11 defines the changing rate of the total cracks area to the total clods area, and it increased with a decreasing sludge moisture content. It measures the degree of shrinkage in the sludge clods to the cracks. At the equilibrium moisture content of 8% dry basis, the total crack area was about 0.96 times the total clod area, which showed that the crack area was almost equal to the clods area when fully dried to it equilibrium moisture content. The crack-clod ratio had a good logarithmic correlation with the sludge moisture content, and high coefficient of determination.

Sludge drying rate encouraged earlier formation of cracks on the sludge surface, and rapid increase in the crack morphological features such as the total crack length, width, crack compactness, and decreased the sludge clod features except the number of clods. All the crack and clod morphological features, except the crack elongation exhibited a significant change in value with changes in the sludge moisture content.

One of the main goal of this research work is

to investigate the relationship between the crack pattern morphological features and the sludge moisture content, and the possibility of using these features for the sludge moisture prediction. To achieve this, the sludge surface crack were analyzed quantitatively and qualitatively. The morphological features extracted from the images were used in formulating several sludge moisture prediction regression models, from which the most appropriate model was selected after validation. The dependent variable was the sludge moisture content, and the independent variables were the crack and clod morphological features with high R^2, that is, crack compactness, crack-clod ratio, clod compactness and number of clods. Stepwise regression selection of the statistical package, Minitab, was then applied to select the best features for the sludge moisture prediction.

The basic problem encountered in regression model selection is to find the model which has a good fit. In this way, model with high R^2 is desired, because it gives the amount of variability in the model. To achieve narrow confidence intervals, and accurate estimates of prediction-moisture content, the mean squared error (MSE) should be small (Dale, *et al.*, 1991). Based on the above criteria, the model developed from experiment B data set (equation 7) was selected for the sludge moisture prediction. With any statistical model, there is usually error involved. In validating its accuracy, validation data was obtained from experiment A data set and cross validation method was applied, by comparing the mean squared error (MSE) obtained from the developed regression model with the mean squared prediction error (MSPR) estimated from the validation data set. From the work of Dale, *et al.* (1991), MSPR was estimated by the relationship :

$$MSPR=\frac{\sum_{i=1}^{n}(Y_i-YP_i)^2}{n} \qquad (5)$$

Where Y_i = the value of the response variable in the i^{th} case of the validation data set.

YP_i = the prediction value for the i^{th} case, based on the substitution of the validation data set in the developed model.

n = the number of data points in the validation data set.

While the MSE value was obtained directly from the regression model fitting by the relationship :

$$MSE=\frac{(Y_i-YP_i)^2}{n-k-1} \qquad (6)$$

Y_i, YP_i, and n are as stated above, and K is the number of independent variables in the model If the MSPR of the validation data is fairly closed to the MSE obtained from the regression fitting, then the MSE for the selected model is not seriously biased, and gives an appropriate indication of the predictive ability of the model (Dale *et al.*, 1991). The selected regression model is thus :

$$Y=-116-4\times10^{-4}X_1^2+306\,X_2^2+0.226\,X_3$$
$$\cdots\cdots\cdots\cdots R^2=0.993 \qquad (7)$$

Where :

Y = Sludge moisture content (% d. b)

X_1 = Crack compactness

X_2 = Crack-clod ratio

X_3 = Clod compactness

The selected model has MSE value of 34.15, with $R^2=0.993$, while from the validation, MSPR was 37.06, for the range of 80-250% moisture content. Table 3 shows the MSE, R^2, and MSPR, estimated for each of the regression model. The large variation between the MSE and the MSPR of the selected model is due to the significant difference in the residuals at different moisture content ranges, especially at very high or very low moisture contents. Fewer cracks developed at extreme high moisture contents, and there was the difficulty in segmentation of cracks from the clods at very low moisture contents ; where crack patterns were very complex and with large number of micro-cracks. Fig. 12. shows the comparison between the predicted and experimental moisture contents.

The agreement between the predicted and

Table 3 The MSE, R^2, MSPR, estimated for each of the regression models

Data for mode formulation	Formulated model	MSE	MSPR	R^2	n
Exp. B data	$Y=-116-4\times10^{-4}X_1^2+306X_2^2+0.226X_3$	34.15	—	0.993	30
Validation with date of exp. A		—	42.16	—	13
Validation with data of exp. A (80-250%)		—	37.06	—	7
Exp. A data	$Y=-886-4\times10^{-4}X_1^2-58X_2^2+0.708X_3$	190.12	—	0.988	13
Validation with date of exp. B		—	246.52	—	30
Validation with data of exp. B (80-250%)		—	256.86	—	26
Exp. B (80-250%) data	$Y=-147-3\times10^{-4}X_1^2+201X_2^2+0.245X_3$	46.88	—	0.986	26
Validation with date of exp. A (80-250%)		—	266.15	—	7
Validation with whole of Experiment A Data		—	233.66	—	13
Exp. A (80-250%) data	$Y=-300-6\times10^{-4}X_1^2+721X_2^2+0.351X_3$	400.90	—	0.958	7
Validation with date of exp. B (80-250%)		—	211.24	—	26
Validation by using the whole data of Exp. B		—	230.08	—	30

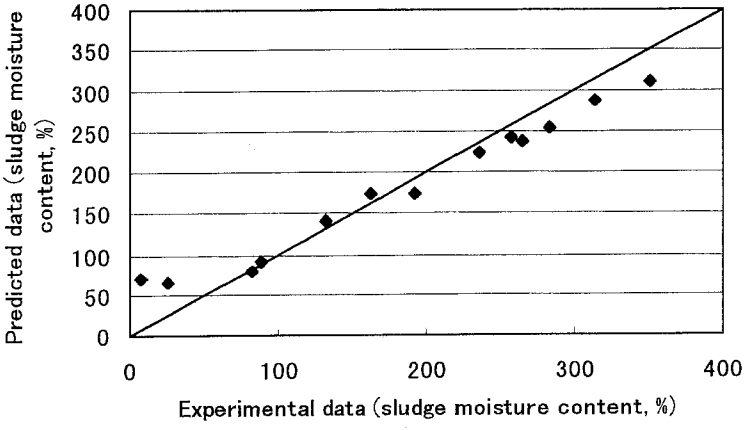

Fig. 12 Comparison between the predicted and experimental moisture contents.

the experimental data using this model appears very good for evaluating the sludge moisture content within the range of 80% to 250% (d. b) moisture contents, as can be seen in Fig. 12. This range, is very important for sludge strengths and traction parameters studies on the sludge surface. From the current studies, at moisture content of 250%, the moisture suction, PF, at 10 cm depth of the sludge surface is 1.30, the average cone resistance, and the average dry bulk density of the depth 0 to 40 cm are 84.71 kPa and 369.28 kg/m^3 respectively. At moisture content of 150%, the PF value is 2.77, average cone resistance, and average dry bulk density of the depth 0 to 40 cm are 843.40 kPa and 486.08 kg/m^3 respectively.

With the developed regression model, the sludge moisture contents can be predicted to a good accuracy within the stated range, but field validation of the model is required for its efficient use in the sludge integrated handling system.

4. Conclusion

The sludge surface crack pattern was analyzed by the technique of image processing at varying sludge moisture content, to extract

the crack and clod morphological features. The features, which were later used in developing a regression model for evaluating the sludge moisture content. From the results of the experiments and the model validation, it shows that the crack and the clod morphological properties can be used to predict the sludge moisture content to a good accuracy within the range of 250% (d. b) to 80% (d. b) moisture content, using the features crack compactness, crack-clod ratio and the clod compactness. The crack features increased with a decrease in the sludge moisture content ; and the clod features, except for the number of clods, decreased with a decrease in sludge moisture content. The crack-clod ratio which measures the degree of shrinkage in the drying sludge increased with a decrease in the sludge moisture content, and as the drying progresses to a lower moisture content, the cracks area was almost equal to the clods area. Crack elongation remains fairly constant with decreasing sludge moisture content, while the crack angle of orientation exhibited a parabolic shape. The crack pattern on the sludge surface was found to depend on the sludge drying rate and moisture content, and the developed regression model performed moderately well under laboratory test, but field validation of the model is required for its efficient use in the sludge integrated handling system.

References

Alan H. Kvanli. (1988) : Statistics, a computer-integrated approach, 8th edition. West Publishing Company ; 50, W. Kellogg Boulevard, Minnesota. USA.

Bodun, P.O., Shibusawa, S., Sasao, A., Sakai, K., Nonaka, H., (2000) : Dredged sludge moisture prediction by textural analysis of the surface image. Journal of terramechanics. Vol. **37**, pp. 3-20.

Bronswijk, J.J.B. (1991) : Relation between vertical soil movements and water content changes in cracking clays. Soil Sc. Soc. Am. Journal., Volume **55**, pp. 1220-1226.

Dale, W.A., Bo S.P., James D.Mc., Yanbo H., (1991) : Ultrasonic signal classification for beef quality grading through neural networks. Automated agriculture for the 21st century, Proceedings of ASAE, pp. 116-125.

Gonzalez R.C. and Woods R.E., (1993) : Digital image processing. Addison-Wesley publishing company, Tokyo.

Horgan, G.W., (1998) : Mathematical morphology for analyzing soil structures from images. European Journal of Soil Sc., Vol. **49**, pp. 161-173.

Ioannis Pitas. (1995) : Digital Image Processing Algorithms. Prentice Hall International Series in Acoustics, Speech and Signal Processing. Prentice hall Europe.

Moran C.J., McBratney A.B. and Koppi A.J., (1989): A rapid method for analysis of soil macropore structure. I. Specimen preparation and digital binary image production. Soil Sc. Soc. Am. Journal. Vol. **53**, pp. 921-928.

Murphy C.P., Bullock P. and Biswell K.J., (1977) : The measurement and characterization of voids in soil thin sections by image analysis. Part II. Applications. Journal of Soil Science, Vol. **28**, pp. 509-518.

Nonaka, H. (1997) : Dredged sludge handling for purification in lake Kasumigaura. Masters thesis. Graduate School of Bio-applications and Systems Engineering, Tokyo University of Agriculture and Technology, Fuchu Shi, Japan.

O'Callaghan J.F. and Loveday, J., (1973) : Qualitative measurement of soil cracking patterns. Pattern recognition, Vol. **5**, pp. 83-98.

Preston S., Griffiths B.S. and Young I.M. (1997) : An investigation into sources of soil crack heterogeneity using fractal geometry. European Journal of Soil Sc.. Vol. **48**, pp. 31-37.

Ringrose-Voase A.J. and Bullock P., (1984) : The automatic recognition and measurement of soil pore types by image analysis and computer programs. Journal of Soil Science. Vol. **35**, pp. 673-684.

Ringrose-Voase A. J. (1987) : A scheme for the quantitative description of soil macrostructure by image analysis. Journal of Soil Science. Vol. **38**, pp. 343-356.

Ringrose-Voase A.J. (1990) : One dimensional image analysis of soil structure. I. Principles. Journal of Soil Science. Vol. **41**, pp. 499-512.

Ringrose-Voase A.J. and Nys C. (1990) : One dimensional image analysis of soil structure. II. Interpretation of parameters with respect to four-forest soil profiles. Journal of Soil Science. Vol. **41**, pp. 513-527.

Scott, G.J.T., Webster, R., Nortcliff, S. (1986) : An

analysis of crack pattern in clay soil : its density and orientation. Journal of Soil Science, Vol. **37**, pp. 653-668.

Shibusawa, S. *et al.*. (1996) : Sludge handling vehicle for purification in lake Kasumigaura. Proc. of the 12th Inter. Conf. ISTVS/Beijing. pp. 394-401.

Waller P.M and Wallender W.W. (1993) : Changes in cracking, water content, and bulk density of salinized swelling clay field soils. Soil science. Vol. **156**, No. 6, pp. 415-423.

浚渫底泥乾燥における水分予測のための亀裂パターン解析

ボードン パトリック*・澁澤 栄*・笹尾 彰**・酒井憲司**

* 東京農工大学大学院生物システム応用科学研究科

** 東京農工大学農学部

要 旨

霞ヶ浦から浚渫される大量の底泥が，水田利用の大区画処理ヤードで天日乾燥固化処理されている。乾燥促進のための機械処理が求められており，底泥乾燥状態と地盤支持力を遠隔予測する必要がある。本研究は，表面情報により底泥乾燥状態を予測することを目的に実施した。

浚渫底泥の乾燥過程においては，乾燥の進行とともに土壌の凝縮が地表面からはじまり，更に3次元的な亀裂網の発生・発達及び大小さまざまな土塊が形成される。本報では，土壌水分変化に対する底泥亀裂と土塊の形態変化の関係を記述するため，亀裂網の幾何学的解析を行った。解析結果より，亀裂の形態特性値は水分減少とともに増大したが，土塊の形態特性値は土塊の数を除いて減少した。8% d.b. の平衡含水比で亀裂の地表断面積が土塊の地表断面積の0.96倍になり，また亀裂/土塊の面積比と含水比との間には相関の高い指数関係が認められた。また底泥の亀裂パターンは乾燥速度と水分状態に依存することを認めた。

受稿年月日：1998年 8 月 5 日
受理年月日：1999年10月15日